

## The preparation of carbon nanotube/poly(ethylene oxide) composites using amphiphilic block copolymers

Chantal Semaan · Gilles Pecastaings ·  
Michèle Schappacher · Alain Soum

Received: 8 February 2011 / Revised: 27 June 2011 / Accepted: 27 June 2011 /

Published online: 7 July 2011

© Springer-Verlag 2011

**Abstract** Polymer/multiwall carbon nanotube (MWCNT) composites were prepared by using amphiphilic block copolymers as dispersant. First, MWCNTs were wrapped with amphiphilic block copolymers in aqueous solution. Poly(ethylene oxide) was selected as the hydrophilic block because of its strong affinity with water while one of the following polymers: poly(ethylene), poly(butadiene), poly(styrene), poly(propylene oxide), or poly(thiophene) was used as the hydrophobic block of the copolymers. The dispersions were characterized by optical microscopy and transmission electron microscopy along with UV–Visible adsorption and dynamic light scattering. Based on the results, we could assess the effect on CNT dispersion quality of both, the molar mass of copolymers, the nature of the hydrophobic block and the length of hydrophilic block. The crystallization behavior of composites prepared from these dispersions was investigated. Results were related to the dispersion of the nanoparticles in the polymer matrix.

**Keywords** Carbon nanotubes · Amphiphilic copolymer · Poly(ethylene oxide) nanocomposite

### Introduction

Graphite, graphene, fullerene, and carbon nanotubes (CNTs) are different varieties of carbon in  $sp^2$  hybridization. CNTs defined by Iijima in 1991 [1] have a unique

---

C. Semaan · G. Pecastaings · A. Soum (✉)

Laboratoire de Chimie des Polymères Organiques, IPB-ENSCBP, Université de Bordeaux,  
16 Avenue Pey-Berland, 33607 Pessac Cedex, France  
e-mail: soum@ipb.fr

M. Schappacher

Laboratoire de Chimie des Polymères Organiques, Centre National de la Recherche Scientifique,  
33607 Pessac Cedex, France

tubular structure with nanometer scale diameters and high length over diameter ratios. Either multi-walled carbon nanotubes (MWCNTs) or single-walled carbon nanotubes (SWCNTs) show amazing mechanical, electrical, and thermal properties [2, 3]. As a result, CNTs are considered to be excellent candidate for many potential applications as catalyst support [4], composite materials [5, 6], conductive films [7], or drug delivery devices [8, 9]. The next generation of high-performance composite materials would certainly benefit from both the numerous properties of CNTs and the processability of polymers [10]. Consequently, one of the most promising field for CNT development is in CNT–polymer composites [11].

In this field, depending on the targeted properties, a large variety of polymers have been explored to form composites with CNTs, such as poly(styrene) [12, 13], poly(vinyl alcohol) [14], poly(epoxy) [15], poly(pyrrole) [16], and many others. However, the scope of CNT applications in practical devices has been hampered by poor dispersion in bulk or solution and weak interfacial bonding with polymer matrices. In order to achieve optimal enhancement in the properties of CNT–polymer composites, two key issues should be considered: homogeneous dispersion of CNTs in solution and uniform distribution of CNTs in the polymer matrix. Usually, this is obtained thanks to CNT functionalization [17].

There are two different approaches to functionalize CNTs: chemical functionalization and non-covalent wrapping methods.

The advantage of the chemical functionalization method is that functional groups are covalently linked to the CNT surface. However, reaction with the graphitic sheets also results in breaking the  $sp^2$  conformation of the carbon atoms and consequently electrical and mechanical properties of the chemically functionalized CNTs can decrease dramatically [18, 19].

The non-covalent dispersion of CNTs involves, using surfactants, oligomers, and polymers, to wrap CNTs and to enhance their solubility [18, 20]. The advantage of the non-covalent method is that the integrity of CNT structure is not disrupted and the intrinsic properties of the CNTs are therefore preserved. Most of the works have been realized in organic solvents but water-soluble polymers such as poly(vinyl-pyrolidone) and poly(styrenesulfonate) have been used to enhance the solubility of CNTs in aqueous solution [20]. Biomolecules such as DNA [21, 22] and helical amylase [23] have also been used to bind CNT or to encapsulate them. In water, using amphiphilic molecules, the solubility of CNTs can be greatly enhanced by anchoring of hydrophobic segments on the surface of CNTs whereas hydrophilic segments are oriented toward the aqueous solution (Fig. 1). In recent years, many groups worked on the dispersion of CNTs using amphiphilic block copolymers [24, 25] but only a few of them discussed on the relationships between the dispersion and the copolymer structure.

In this work, we describe both, a non-covalent process for surface functionalization of MWCNTs using amphiphilic block copolymers and the characterization of the corresponding dispersions. The hydrophilic block was made of poly(ethylene oxide) (PEO) and the hydrophobic block of poly(ethylene) (PE), poly(styrene) (PS), poly(propylene oxide) (PPO), poly(butadiene) (PBut), or poly(thiophene) (PT). PEO is a semicrystalline polymer that has been used in many applications of biomedical [26, 27] and electrochemical [28] domains. It has been chosen as a model of

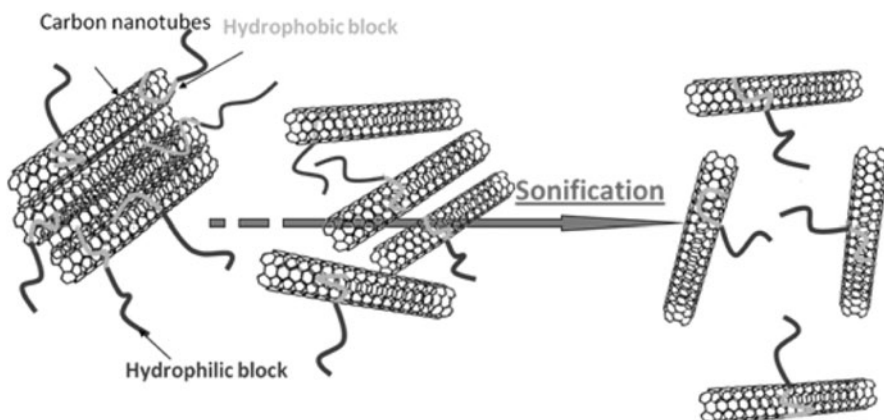


**Fig. 1** Representation of CNT aqueous dispersion through wrapping by amphiphilic block copolymers polymer matrix since it is water soluble and consequently allows the preparation of polymer composites without the use of organic solvent.

## Experimental

### Materials

The MWCNTs used in this study are Graphistrength® supplied by Arkema and prepared by Catalytic Chemical Vapor Deposition (CCVD) [29, 30]. They have an outer diameter within the range 12–20 nm and an initial average length between 1 and 10  $\mu\text{m}$ . Their pristine chemical composition is presented in Table 1.

The amphiphilic block copolymers were supplied either by polymer source (PS–PEO, PBut–PEO, PPO–POE) or Aldrich (PE–PEO). The copolymer poly(PT–PEO) was synthesized according to the method reported by Lee et al. [31]. Their molar mass and their composition were checked by NMR and SEC and are reported in Table 3. The polymer used as matrix is a PEO ( $M_n = 14,000$  g/mol, PDI = 4.6 supplied by Aldrich).

### Preparation of MWCNT aqueous suspensions and polymer composites

MWCNTs were purified using acid treatment with sulfuric ( $\text{H}_2\text{SO}_4$ ) or nitric ( $\text{HNO}_3$ ) acids to remove carbonaceous impurities and metal catalyst particles

**Table 1** Composition of pristine MWCNTs

Atoms	Content (at.%)
Fe <sup>a</sup>	2.01
Al <sup>a</sup>	2.62
C <sup>b</sup>	95
H <sup>b</sup>	0.2
O <sup>b</sup>	0.3

<sup>a</sup> Determined by chemical analysis

<sup>b</sup> Determined by XPS

[32–34]. In a typical experiment, 10 g of MWCNTs were refluxed for 5 h in 100 mL of 3.6 M  $\text{H}_2\text{SO}_4$  aqueous solution. With  $\text{HNO}_3$ , 5 g of MWCNTs were refluxed for 24 h in 500 mL of 2 M, 4 or 6 M  $\text{HNO}_3$  solution. The mixture was then cooled down to ambient temperature and MWCNTs were filtered, washed with copious amounts of pure water until the pH value of the solution became neutral. Finally MWCNTs were stored in solution at 90% of water. This value was checked by thermogravimetric analyses.

Dispersions were prepared by mixing wet MWCNTs with an aqueous solution of amphiphilic block copolymers. In a typical experiment, 50 mg of 10 wt% MWCNT aqueous solution (5 mg MWCNTs) were mixed with 20 mg of copolymer dissolved in 5 mL of water. The mixture was sonicated for 15 min at 15 W using an ultrasonic probe (Vibra Cell model 75186) [35, 36].

The resulting dispersions were then used to prepare composite materials with a polymer matrix made of PEO. Typically, for 1 wt% MWCNT composite, 950 mg of PEO was mixed with wrapped NTCs (10 mg of dried MWCNTs and 40 mg of copolymer), over 24 h at 70 °C. The mixture was then evaporated at room temperature for 3 or 4 days and post-cured under vacuum during 48 h at 50 °C then 24 h at 120 °C.

#### Characterizations and measurements

Morphology and homogeneity of MWCNT solutions obtained with different concentrations of CNTs and copolymers were analyzed using various techniques described below.

Thermogravimetric analyses (TGA) were realized on a Q500 apparatus from TA Instruments with a heating rate of 20 °C/min from 20 to 900 °C.

X-ray photoelectron spectroscopy (XPS) measurements were made using an Escalab 220-iXL spectrometer (Thermo-Electron, VG Company) in an ultra high vacuum. Photoemission was stimulated by monochromatized Al Kr radiation (1486.6 eV). Survey scan data was collected using a pass-energy of 20 eV. An area of about 250  $\mu\text{m}$  diameter was analyzed for each sample. Surveys and high-resolution spectra were recorded and then fitted with an Avantage processing program provided by ThermoFisher Scientific.

Chemical analyses were realized by the CNRS Central Laboratory.

In optical microscopy (OM) experiments, the solutions were placed between glass slides and observed under a Zeiss Axioskop 40 microscope in transmission polarized mode equipped with a 40 $\times$  objective. The total area analyzed was 576  $\text{mm}^2$  (24 mm  $\times$  24 mm).

UV-visible analyses were carried out on a Varian Cary 3E between 200 and 800 nm on initial aqueous solutions of copolymer wrapped MWCNTs without any dilution.

The TEM images were obtained on a Hitachi H7650. Samples were prepared placing a drop of solution onto a carbon-coated copper grid. About 2 min later, surface water was removed from the grid with filter paper and samples were dried in air at room temperature. In the case of composite materials, thin solid samples were prepared by cryomicrotomy. The usual thickness was around 50 nm.

Dynamic light scattering (DLS) measurements were performed to determine the dimensions of CNTs in aqueous suspension. The length and the diameter of CNTs were calculated with the model described by Badaire et al. [37]. The temporal autocorrelation function of the scattered light was measured with a Brookhaven digital correlator. A coherent laser operating at 532 nm was used as the excitation source. The scattered intensity polarized in the horizontal direction was detected for scattering angles between 40 and 100°. The samples were equilibrated 2 weeks before any measurement to allow large dust particles possibly present to sediment.

Differential scanning calorimetry (DSC) analyses were performed with a Q1000 apparatus from TA Instruments, on PEO matrix containing various concentrations of CNTs with or without copolymer wrapping. The analyses were carried out in a nitrogen atmosphere with aluminum pans. The following procedure was used: the system was first heated at 5 °C/min between 25 and 140 °C (first heating) and kept at 140 °C for 20 min to ensure complete melting of the sample. The melted sample was then cooled rapidly (60 °C/min) to 40 °C, for the isothermal crystallization studies, kept for 10 min at the temperature and then heated to 140 °C at a rate of 5 °C/min (second heating). Finally the sample was cooled to 25 °C at a rate of 5 °C/min (cooling).

The critical micellar concentration (CMC) of amphiphilic block copolymers was measured using fluorescence spectroscopy according to the method first described by Kalyanasundaram and Thomas [38]. In a typical experiment, pyrene was dissolved in ethanol at the concentration of  $4 \times 10^{-4}$  M. Then, 25  $\mu$ L of this solution was introduced into a plastic microtube and ethanol was evaporated. An aliquot of an aqueous solution of amphiphilic block copolymer in water, at various concentrations, was added to obtain a final concentration of  $5 \times 10^{-6}$  M pyrene. Fluorescence spectra of pyrene were obtained at the excitation wavelength of 339 nm and at the emission wavelength of 390 nm on a spectrofluorometer Eclipse from Cary. The CMC values were calculated plotting the emission absorbance ratio (I373/I393) and the excitation absorbance ratio (I339/I333) versus copolymer concentration ranging from  $10^{-2}$  to  $10^{-5}$  wt%.

Hydrodynamic radius ( $R_H$ ) and dispersity for different amphiphilic block copolymers were measured by DLS at 90° and the autocorrelation function was fitted with the cumulant method. The experiments were carried out using an ALV laser goniometer which consisted of a 35 mW He–Ne linear polarized laser with a wavelength of 632.8 nm and an ALV-5000/EPP Multiple Tau Digital correlator. Samples were kept at constant temperature (25 °C) during the experiments. Typical copolymer concentrations were about 0.25 wt%.

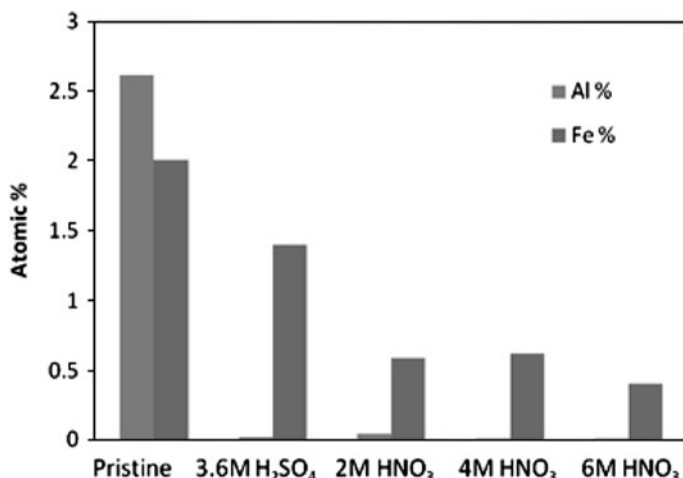
## Results and discussion

### Purification of MWCNTs

The total weight fraction of impurities (mainly catalyst residues) of pristine MWCNTs (Graphistrength®) usually ranges from 5 to 15 wt% [39]. In order to

**Table 2** Composition of pristine MWCNTs and purified MWCNTs determined by XPS

MWCNT samples	Acid concentration (M)	Carbon content (at.%)	Oxygen content (at.%)
Pristine		99.7	0.3
Purified with $\text{H}_2\text{SO}_4$	3.6	98.8	1.2
Purified with $\text{HNO}_3$	2	96.1	3.9
	4	95.3	4.7
	6	94.2	5.8

**Fig. 2** Amount (measured by chemical analysis) of catalyst metal atoms (Fe, Al) contained in pristine MWCNTs and MWCNTs treated with sulfuric and nitric acids

eliminate these residues, the pristine carbon nanotubes were purified by either  $\text{H}_2\text{SO}_4$  or  $\text{HNO}_3$  treatment. Additionally, as previously reported in the literature [40], such treatment increases the oxygen amount on the nanotube surface and is supposed to facilitate the dispersion. As shown in Table 2 and Fig. 2, whatever the acid, the amount of impurity decreases with the treatment. On the contrary, the amount of oxygen on carbon nanotube surface increases from  $\text{H}_2\text{SO}_4$  to  $\text{HNO}_3$  treatment. Furthermore, with  $\text{HNO}_3$ , the amount of oxygen increases drastically with the acid concentration. Nevertheless, as indicated by TGA analysis (Fig. 3), the MWCNT stability decreased from sulfuric to nitric acid treatment and with increasing nitric acid concentration. This let suppose a significant deterioration of CNT sidewalls in reaction with nitric acid. Therefore, considering the nitric acid effect and that we did not observe significant differences in the dispersion ability as a function of acid nature, the results reported hereafter were obtained with MWCNTs purified with sulfuric acid, as described in the “Experimental” section.

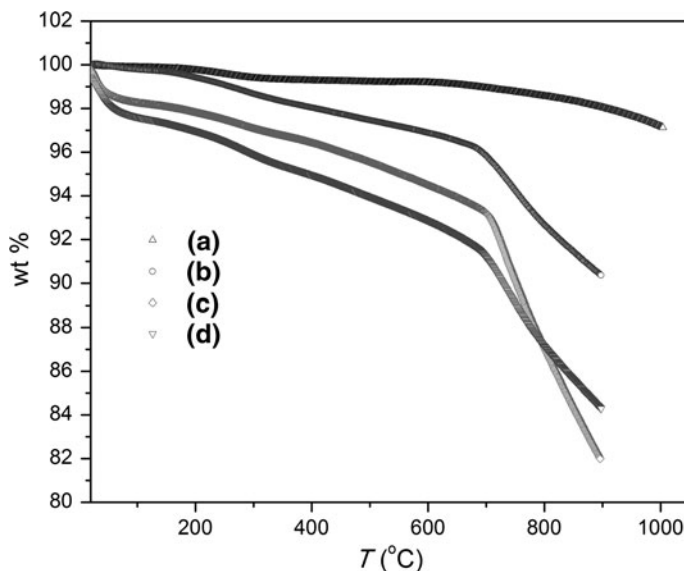


**Fig. 3** Weight loss of purified MWCNTs versus temperature measured by TGA: treatment in (a) 3.6 M boiling sulfuric acid; (b) 2 M, (c) 4 M, and (d) 6 M boiling nitric acid

#### Aqueous dispersions

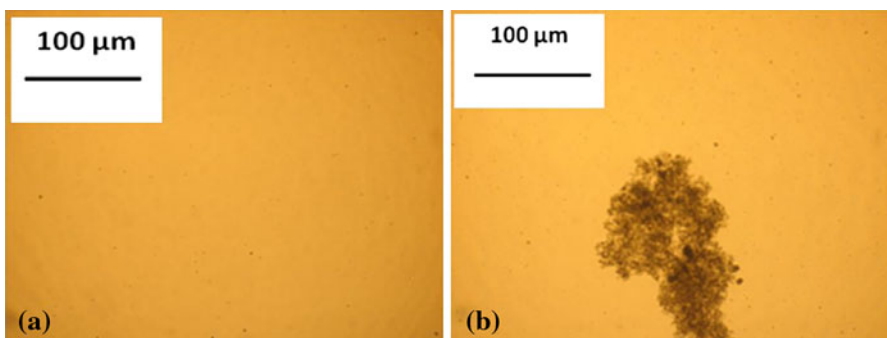
In preliminary experiments, with the objective to evaluate the effect of the chemical structure of the hydrophobic block on the dispersion homogeneity, various amphiphilic block copolymers were used to wrap MWCNTs. As shown in Table 3, the block copolymers **1**, **2**, **3**, and **4** have approximately the same length (total molar mass) and the same composition. Optical microscopic observations (Fig. 4) indicate that dispersions made with block copolymers **1** and **2** are homogeneous and stable with time contrarily to those made with block copolymers **3** and **4** which reaggregate within 1 week or 3 months respectively. This indicates that the dispersion ability of copolymers depends on the chemical structure of the hydrophobic block.

As suggested previously in this article, two other characteristics of the block copolymers may influence their efficiency in dispersing MWCNT: the molar mass and the molar composition which determine, for a given total length of the copolymer, the length of each block and the hydrophilic/hydrophobic balance. As shown in Table 3, for a given composition (polymers **3**, **6** and polymers **2**, **5**) the increase of the copolymer length appears to decrease the dispersion quality. Contrarily, whatever the total length, the increase of hydrophilic moiety, increases the efficiency of the copolymer as in the case of polymers **6** and **7**. It is also noteworthy that PT-PEO copolymer (**8**) with a high hydrophilic/hydrophobic balance is very efficient to disperse MWCNTs.

Further evidence of the dispersion state of the different solutions is provided by UV–Visible adsorption (Figs. 5, 6). Indeed, the absorption of MWCNT aqueous solutions depends on the number of nanotubes homogeneously dispersed in water.

**Table 3** Optical microscopy observations of dispersions of MWCNTs with different amphiphilic blocks copolymers

Number	Block copolymers	Molar mass (g/mol) <sup>a</sup>	Composition of blocks (mol.%) <sup>b</sup>	Dispersion state <sup>c</sup>	
				1 week after	3 months after
<b>1</b>	PE–PEO	4,000	23–76	No aggregation	
<b>2</b>	PPO–PEO	5,200	27–73	No aggregation	
<b>3</b>	PS–PEO	6,700	22–78	No aggregation	Aggregation
<b>4</b>	PBut–PEO	4,500	28–72	Aggregation	
<b>5</b>	PPO–PEO	10,200	28–72	Aggregation	
<b>6</b>	PS–PEO	19,000	30–70	Aggregation	
<b>7</b>	PS–PEO	28,600	5–95	No aggregation	
<b>8</b>	PT–PEO	2,738	14–86	No aggregation	

<sup>a</sup> Determined by size exclusion chromatography<sup>b</sup> Determined by <sup>1</sup>H NMR<sup>c</sup> Observed by optical microscopy**Fig. 4** OM images (3 months after sonification) of aqueous dispersions of 0.1 wt% MWCNTs in: **a** 0.25 wt% PE–PEO **1** (no presence of aggregation), **b** 0.25 wt% PS–PEO **3** (presence of aggregation)

So, the absorption level of the dispersions can be related to the homogeneity of the solutions. As observed previously by optical microscopy, PE–PEO (polymer **1**) and PPO–PEO (polymer **2**) appeared to be the most efficient copolymers (Fig. **5**). The same observation can be made within the PS–PEO copolymer series: PS–PEO with the larger hydrophilic block (polymer **7**) is the most efficient as shown in Fig. **6**.

So, all the results indicate that, surprisingly, the dispersion efficiency of the block copolymers is higher with those which exhibit lower interaction potentialities with MWCNTs (PE–PEO; PPO–PEO; short PS blocks) than with the copolymers which can interact strongly with CNTs (PS–PEO; PBut–PEO).

This let suppose that the driving force of the dispersion is a non-specific interaction between the absorbing block (hydrophobic block) and the tube. This agrees with a mode of interaction between dispersing copolymers and CNTs

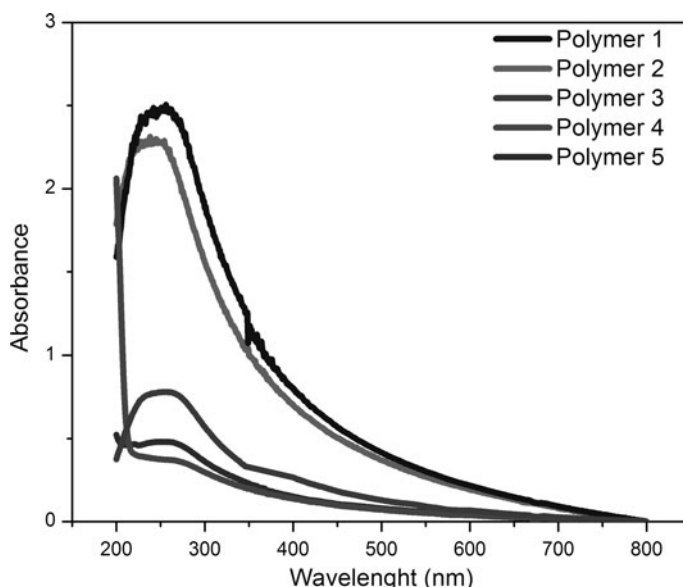


**Fig. 5** UV–Visible absorption spectra (1 week after sonification) of 0.05 wt% MWCNT aqueous solutions with 0.25 wt% of PE–PEO **1**, PPO–PEO **2**, PBut–POE **4**, and PPO–PEO **5** block copolymers

described by a non-wrapping model as previously reported for PEO–PPO–PEO triblock copolymers [41].

This is confirmed by the fact that the variations of the quality of the MWCNT dispersions (homogeneity, stability) with the chemical structure and the composition of the block copolymers may be correlated to the lower or higher self-assembling ability of such copolymers in aqueous solution, such ability depending as known [42], on copolymer structure. Indeed, although in all experiments block copolymer concentrations are always over the CMC, as shown in Table 4, the amphiphilic copolymers which are the most efficient in MWCNT dispersion (**1**, **2**, **7**, and **8**) give the less stable micelles (both higher hydrodynamic radius and higher polydispersity). As already mentioned [43], the micelle steric stabilization depends not only on the composition (hydrophilic/hydrophobic balance) but rather on the length of the polar block. As an example, for the same balance and chemical structure, copolymers **5** and **6** which exhibit the longer polar PEO block, give more stable micelles than copolymers **2** and **3** and therefore, are less efficient for the dispersion. So, with copolymers which give micelles of poor stability, under sonification, the micelles are more or less rapidly destroyed and the CNTs are decorated by the copolymer before their re-aggregation as bundles. Therefore, the number of CNTs homogeneously dispersed depends on the equilibrium between the micelles and the isolated copolymer chains.

In the case of copolymer **8** which exhibits a high hydrophilic balance, the high efficiency in dispersion may be related to the specific strong interactions [31]

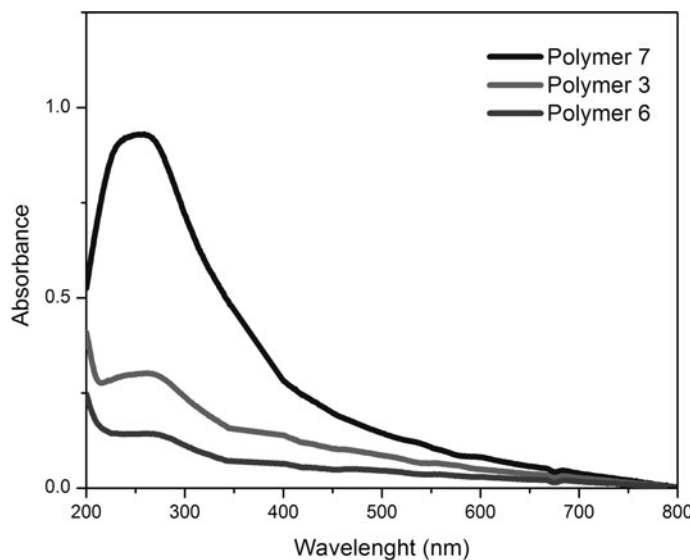


**Fig. 6** UV–Visible absorption spectra (3 months after sonification) of 0.05 wt% MWCNT aqueous solutions with 0.25 wt% of PS–PEO **3**, PS–PEO **6**, and PS–PEO **7** amphiphilic block copolymers

**Table 4** Characteristics of self-assembled block copolymers in water (0.25 wt%)

Number	Block copolymers	Radius (nm) <sup>a</sup>	Polydispersity <sup>a</sup>	CMC (wt%) <sup>b</sup>
<b>1</b>	PE–PEO	75	0.44	$\sim 10^{-4}$
<b>2</b>	PPO–PEO	104	0.35	$\sim 5 \times 10^{-2}$
<b>3</b>	PS–PEO	49	0.22	–
<b>4</b>	PBut–PEO	24	0.30	–
<b>5</b>	PPO–PEO	27	0.30	$\sim 10^{-3}$
<b>6</b>	PS–PEO	59	0.23	–
<b>7</b>	PS–PEO	75	0.46	$\sim 10^{-4}$
<b>8</b>	PT–PEO	78	0.35	–

<sup>a</sup> Determined by DLS (see “[Experimental](#)” section)

<sup>b</sup> Determined by fluorescence spectroscopy (see “[Experimental](#)” section)

possible between poly(thiophene) block and MWCNT. In this case, such interactions would be the driving force of the dispersion.

The decoration of the MWCNTs by the copolymers is confirmed by transmission electron microscopy (TEM) (Fig. [7](#)). Indeed, TEM images of crude MWCNTs indicate an average diameter of around 18 nm (Fig. [7a](#)) whereas MWCNTs dispersed in the presence of block copolymers appears to be coated with a polymer layer and the average CNT diameters range from 22 to 35 nm depending on the dispersing copolymers (Fig. [7b–e](#)).

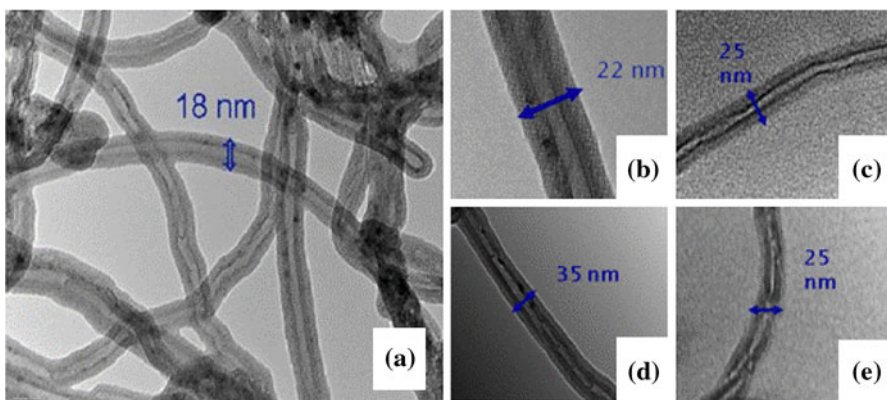


**Fig. 7** TEM images of MWCNT dispersions: **a** without copolymer, **b** wrapped with PE-PEO **1**, **c** wrapped with PPO-PEO **2**, **d** wrapped with PBut-PEO **4**, **e** wrapped with PS-PEO **3**

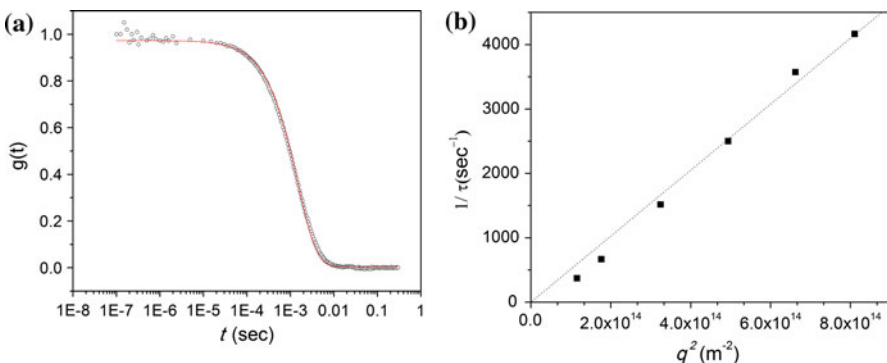


**Fig. 8** DLS characterization of MWCNTs wrapped with PPO-PEO **3** in aqueous solution (0.02 wt%): **a** example of depolarized DLS time correlation function at 90°, **b** variations of  $1/\tau$  versus  $q^2$  and linear fit  $1/\tau = 5.12 \times 10^{-12} q^2$

The systems stabilized by PPO-PEO (polymer **2**) are perfectly homogenous and can be therefore characterized by DLS measurements. Using the same procedure as previously reported [37], we measured the depolarized components of the scattered light using dilute suspensions leading to the calculations of the translational and rotational Brownian diffusion coefficients (Fig. 8). From these diffusion coefficients, considering the nanotubes as rigid rods and using the Broersma equations [44], both the average length  $L$  and the average diameter  $D$  of the nanotubes can be calculated. The values are  $L = 250 \pm 70$  nm and  $D = 40 \pm 5$  nm. The measured length is lower than the initial average length (1–10  $\mu$ m) which is usual when dispersions are made by sonication [39]. The measured diameter is larger than the diameter deduced from TEM observations of wet and dried MWCNTs. This difference is not surprising since the copolymer in solution is expected to be swollen. Moreover, dynamic light scattering gives hydrodynamic diameter which is always to some extent, larger than the actual one (because it includes the hydration

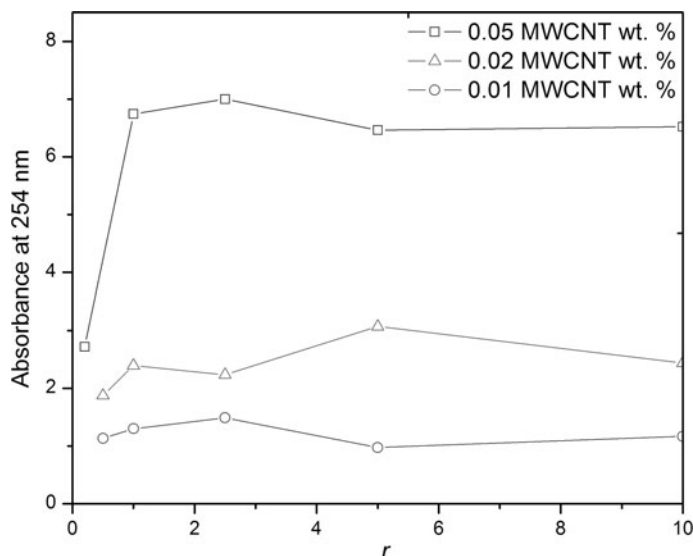


**Fig. 9** Variations of UV–Visible absorption at 254 nm of MWCNT aqueous solutions versus the ratio  $r$  of copolymer **1** ( $r = [\text{wt\% of amphiphilic block copolymer PE–PEO}]/[\text{wt\% of MWCNT}]$ )

layer). Despite these differences, this *in situ* experiment confirms that MWCNTs are coated with a regular layer of copolymer.

Finally, with copolymer **1** (PE–PEO) as wrapping polymer, we analyzed the effect of the concentration of block copolymer on the dispersion quality (Fig. 9). Within experimental error, these results indicate that for a ratio  $r$  over 1 ( $r = [\text{copolymer}/\text{MWCNT}]$ ) which is necessary to give homogeneous dispersion, there is no effect of the copolymer concentration.

Hence, for further preparation of polymer composites, we chose a concentration of amphiphilic block copolymers of 10 wt% which allows varying MWCNT concentrations from 0.05 to 9 wt% with a ratio always over 1.

#### Crystallization behavior of MWCNT poly(ethylene oxide) composites

It is well known that the crystallization behavior of semi-crystalline polymers is affected by the presence of fillers since it depends on two factors: the entropic contribution to the free energy of formation of a nucleus of critical dimension to be stable and the energy required for the transport (diffusion) to the growth front [45]. Consequently, the variations of such behavior in the presence of nanotubes may be an image of their dispersion in the polymer matrix. With this objective, we studied the crystallization of PEO matrix filled with unwrapped and wrapped MWCNTs by DSC, according to the procedure described in “**Experimental**” section.

The effect of MWCNT content on crystallization is shown in Fig. 10 which presents the variations, with MWCNT ratio, of the relative percentage of crystallinity ( $X_c$ ) defined as:

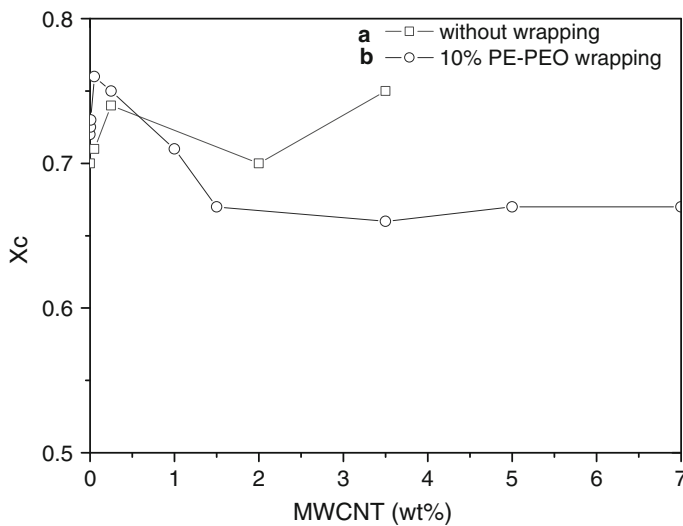


**Fig. 10** Variation of crystallinity ratio  $X_c$  with MWCNT content in PEO–MWCNT composites: (a) without copolymer wrapping (b) with 10 wt% PE–PEO **1** wrapping

$$X_c = \frac{\Delta h_c}{(1 - \alpha)\Delta h_f^0}$$

with “ $\alpha$ ” the fraction of fillers in the PEO matrix,  $\Delta h_f^0$  the enthalpy of 100% crystalline PEO (205 J/g from Ref. [46]) and  $\Delta h_c$  the measured enthalpy from DSC.

At low wrapped and unwrapped MWCNT content, the crystallinity increases compared to that of pure PEO ( $X_c^0 = 0.70$ ). Then, at higher CNT concentrations (>0.25 wt%), with wrapped MWCNTs, the crystallinity decreases until a value lower than those of pure PEO whereas it remains almost unchanged (within experimental error) with unwrapped MWCNTs.

At low concentration, it can be reasonably assumed that MWCNTs act as seeds and so accelerate the nucleation [47, 48]. Consequently, with both defined time and temperature of crystallization, the amount of crystalline part increases. Contrarily, at higher concentrations, the presence of MWCNTs well dispersed in the matrix may decrease the mobility (transport to growth front) and consequently the crystallinity decreases as observed previously by Chatterjee et al. [49]. With unwrapped MWCNTs, the nanotubes are mostly present in the matrix as bundles and therefore, since there is a large domain without fillers in PEO matrix, the crystallinity may not be so much affected (Fig. 11). With wrapped MWCNTs homogeneously dispersed, the viscosity of all the PEO matrix increases and consequently, the crystallization possibilities decrease.

TEM image (Fig. 12) of a nanocomposite made with 3.5 wt% of MWCNTs wrapped with 10 wt% of PE–PEO copolymer (**1**) and a PEO matrix, confirms the dispersion of CNTs all over most of the matrix domains.

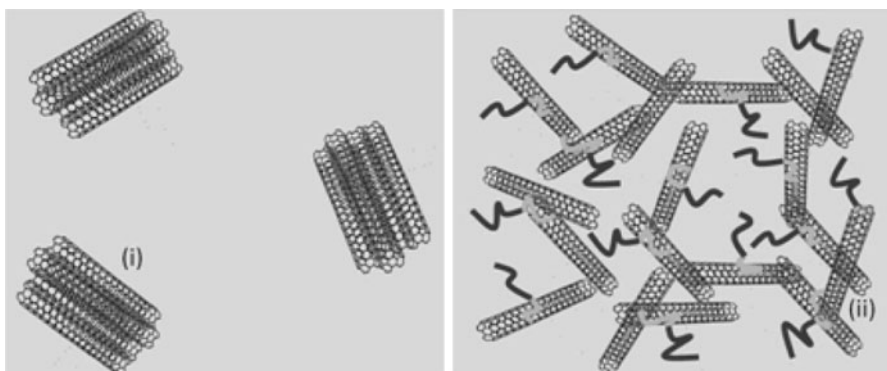


**Fig. 11** Representation of MWCNTs dispersed in PEO matrix: **i** bundles of unwrapped MWCNTs in PEO matrix, **ii** network of wrapped MWCNTs in PEO matrix

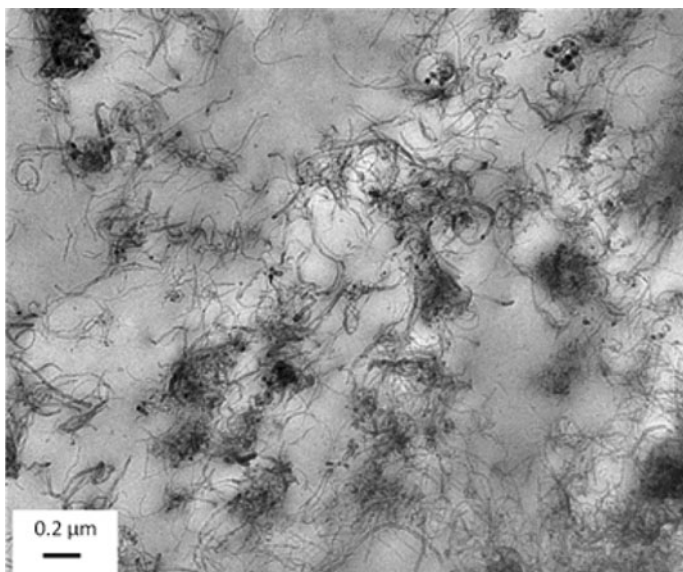


**Fig. 12** TEM image of PEO composite with 3.5 wt% MWCNTs wrapped with 10 wt% of PE-POE 1

## Conclusion

We have demonstrated the efficiency of amphiphilic block copolymers to wrap MWCNTs and dispersed them in aqueous solution. This efficiency has been related to the structure of the copolymers (chemical composition, molecular weight, hydrophilic/hydrophobic balance). Particularly, we demonstrated that the more the micelles are stable, the less the copolymer is efficient for dispersion, this micelle stability being influenced by the structure of the copolymer. This agrees with a mechanism of wrapping based on a weak (non-specific) interaction between

MWCNTs and hydrophobic part of the copolymer. In this way, among the copolymers evaluated, PE–PEO, PPO–PEO, and PT–PEO block copolymers are the most efficient for the dispersion of MWCNTs in aqueous phase. TEM analysis confirms that the nanotubes are decorated with a layer of block copolymer. We have also shown that UV–Visible absorption of solution and crystallization ratio can be related to the homogeneity of the dispersions. Further evaluation of the properties of composites filled with MWCNTs wrapped through the method described in this article, is in progress and will be published soon.

**Acknowledgments** We acknowledge financial support from ARKEMA group and Region Aquitaine. We thank Dr. Philippe Poulin, Dr. Cecile Zakri and Maryse Maugey from CRPP-CNRS-Bordeaux for useful discussions on DLS characterization methods, Christine Labrugère from ICMCB-CNRS-Bordeaux for XPS analysis and Bordeaux Imaging Center for TEM observations.

## References

1. Iijima S (1991) Helical microtubules of graphitic carbon. *Nature* 354:56–58
2. Poncharal P, Wang ZL, Ugarte D, de Heer WA (1999) Electrostatic deflections and electromechanical resonances of carbon nanotubes. *Science* 283(5407):1513–1516. doi:[10.1126/science.283.5407.1513](https://doi.org/10.1126/science.283.5407.1513)
3. Collins PG, Avouris P (2000) Nanotubes for electronics. *Sci Am* 283(6):62–69
4. Pan X, Fan Z, Chen W, Ding Y, Luo H, Bao X (2007) Enhanced ethanol production inside carbon-nanotube reactors containing catalytic particles. *Nat Mater* 6(7):507–511
5. Calvert P (1999) Nanotube composites: a recipe for strength. *Nature* 399(6733):210–211
6. Steurer P, Wissert R, Thomann R, Mülhaupt R (2009) Functionalized graphenes and thermoplastic nanocomposites based upon expanded graphite oxide. *Macromol Rapid Commun* 30(4–5):316–327
7. Wu Z, Chen Z, Du X, Logan JM, Sippel J, Nikolou M, Kamaras K, Reynolds JR, Tanner DB, Hebard AF, Rinzler AG (2004) Transparent, conductive carbon nanotube films. *Science* 305(5688):1273–1276. doi:[10.1126/science.1101243](https://doi.org/10.1126/science.1101243)
8. Lu F, Gu L, Meziani MJ, Wang X, Luo PG, Veca LM, Cao L, Sun Y-P (2009) Advances in bioapplications of carbon nanotubes. *Adv Mater* (Weinheim, Germany) 21(2):139–152
9. Pastorin G (2009) Crucial functionalizations of carbon nanotubes for improved drug delivery: a valuable option? *Pharm Res* 26(4):746–769
10. Lin Y, Meziani MJ, Sun Y-P (2007) Functionalized carbon nanotubes for polymeric nanocomposites. *J Mater Chem* 17(12):1143–1148
11. Moniruzzaman M, Winey KI (2006) Polymer nanocomposites containing carbon nanotubes. *Macromolecules* 39(16):5194–5205. doi:[10.1021/ma060733p](https://doi.org/10.1021/ma060733p)
12. Besancon BM, Green PF (2005) Polystyrene-based single-walled carbon nanotube nanocomposite thin films: dynamics of structural instabilities. *Macromolecules* 38(1):110–115. doi:[10.1021/ma049008+](https://doi.org/10.1021/ma049008+)
13. Ugur S, Yargi Ö, Pekcan Ö (2010) Conductivity percolation of carbon nanotubes (CNT) in polystyrene (PS) latex film. *Can J Chem* 88(3):267–276
14. Milo SP, Shaffer AHW (1999) Fabrication and characterization of carbon nanotube/poly(vinyl alcohol) composites. *Adv Mater* (Weinheim, Germany) 11(11):937–941
15. Pecastaings G, Delhaes G, Derre P, Saadaoui A, Carmona H, Cui F (2004) Role of interfacial effects in carbon nanotube/epoxy nanocomposite behavior. *J Nanosci Nanotechnol* 4:838–843
16. Chen GZ, Shaffer MSP, Coleby D, Dixon G, Zhou W, Fray DJ, Windle AH (2000) Carbon nanotube and polypyrrole composites: coating and doping. *Adv Mater* (Weinheim, Germany) 12(7):522–526
17. Chang TE, Jensen LR, Kisliuk A, Pipes RB, Pyrz R, Sokolov AP (2005) Microscopic mechanism of reinforcement in single-wall carbon nanotube/polypropylene nanocomposite. *Polymer* 46(2):439–444
18. Andreas H (2002) Functionalization of single-walled carbon nanotubes. *Angew Chem* 41(11):1853–1859

19. Barber AH, Cohen SR, Wagner HD (2003) Measurement of carbon nanotube–polymer interfacial strength. *Appl Phys Lett* 82(23):4140–4142
20. O’Connell MJ, Boul P, Ericson LM, Huffman C, Wang Y, Haroz E, Kuper C, Tour J, Ausman KD, Smalley RE (2001) Reversible water-solubilization of single-walled carbon nanotubes by polymer wrapping. *Chem Phys Lett* 342(3–4):265–271
21. Zheng M, Jagota A, Semke ED, Diner BA, McLean RS, Lustig SR, Richardson RE, Tassi NG (2003) DNA-assisted dispersion and separation of carbon nanotubes. *Nat Mater* 2(5):338–342
22. Zheng M, Jagota A, Strano MS, Santos AP, Barone P, Chou SG, Diner BA, Dresselhaus MS, McLean RS, Onoa GB, Samsonidze GG, Semke ED, Usrey M, Walls DJ (2003) Structure-based carbon nanotube sorting by sequence-dependent DNA assembly. *Science* 302(5650):1545–1548. doi: [10.1126/science.1091911](https://doi.org/10.1126/science.1091911)
23. Kim O-K, Je J, Baldwin JW, Kooi S, Pehrsson PE, Buckley LJ (2003) Solubilization of single-wall carbon nanotubes by supramolecular encapsulation of helical amylose. *J Am Chem Soc* 125(15): 4426–4427. doi: [10.1021/ja029233b](https://doi.org/10.1021/ja029233b)
24. Richard C, Balavoine F, Schultz P, Ebbesen TW, Mioskowski C (2003) Supramolecular self-assembly of lipid derivatives on carbon nanotubes. *Science* 300(5620):775–778. doi: [10.1126/science.1080848](https://doi.org/10.1126/science.1080848)
25. Park C, Lee S, Lee JH, Lim J, Lee SC, Park M, Lee S-S, Kim J, Park CR, Kim C (2007) Controlled assembly of carbon nanotubes encapsulated with amphiphilic block copolymer. *Carbon* 45(10): 2072–2078
26. Alcantar NA, Aydil ES, Israelachvili JN (2000) Polyethylene glycol-coated biocompatible surfaces. *J Biomed Mater Res* 51(3):343–351
27. Cheng J, Fernando KAS, Veca LM, Sun Y-P, Lamond AI, Lam YW, Cheng SH (2008) Reversible accumulation of PEGylated single-walled carbon nanotubes in the mammalian nucleus. *ACS Nano* 2(10):2085–2094. doi: [10.1021/nn800461u](https://doi.org/10.1021/nn800461u)
28. Aranda P, Mosquera Y, Pérez-Capé E, Ruiz-Hitzky E (2003) Electrical characterization of poly(ethylene oxide)-clay nanocomposites prepared by microwave irradiation. *J Polym Sci Part B: Polym Phys* 41(24):3249–3263
29. Kitiyanan B, Alvarez WE, Harwell JH, Resasco DE (2000) Controlled production of single-wall carbon nanotubes by catalytic decomposition of CO on bimetallic Co-Mo catalysts. *Chem Phys Lett* 317(3–5):497–503
30. Philippe R, Caussat B, Falqui A, Kihn Y, Kalck P, Bordère S, Plee D, Gaillard P, Bernard D, Serp P (2009) An original growth mode of MWCNTs on alumina supported iron catalysts. *J Catal* 263(2):345–358
31. Lee JU, Huh J, Kim KH, Park C, Jo WH (2007) Aqueous suspension of carbon nanotubes via non-covalent functionalization with oligothiophene-terminated poly(ethylene glycol). *Carbon* 45(5): 1051–1057
32. Hou P-X, Liu C, Cheng H-M (2008) Purification of carbon nanotubes. *Carbon* 46(15):2003–2025
33. Vairavapandian D, Vichchulada P, Lay MD (2008) Preparation and modification of carbon nanotubes: review of recent advances and applications in catalysis and sensing. *Anal Chim Acta* 626(2):119–129
34. Tohji K, Takahashi H, Shinoda Y, Shimizu N, Jeyadevan B, Matsuoka I, Saito Y, Kasuya A, Ito S, Nishina Y (1997) Purification procedure for single-walled nanotubes. *J Phys Chem B* 101(11): 1974–1978. doi: [10.1021/jp962888c](https://doi.org/10.1021/jp962888c)
35. Ahir SV, Huang YY, Terentjev EM (2008) Polymers with aligned carbon nanotubes: active composite materials. *Polymer* 49(18):3841–3854
36. Hilding J, Grulke EA, Zhang ZG, Lockwood F (2003) Dispersion of carbon nanotubes in liquids. *J Dispersion Sci Technol* 24(1):1–41
37. Badaire S, Poulin P, Maugey M, Zakri C (2004) In situ measurements of nanotube dimensions in suspensions by depolarized dynamic light scattering. *Langmuir* 20(24):10367–10370. doi: [10.1021/la049096r](https://doi.org/10.1021/la049096r)
38. Kalyanasundaram K, Thomas JK (1977) Environmental effects on vibronic band intensities in pyrene monomer fluorescence and their application in studies of micellar systems. *J Am Chem Soc* 99(7):2039–2044. doi: [10.1021/ja00449a004](https://doi.org/10.1021/ja00449a004)
39. Lucas A, Zakri Cc, Maugey M, Pasquali M, Schoot Pvd, Poulin P (2009) Kinetics of nanotube and microfiber scission under sonication. *J Phys Chem C* 113(48):20599–20605. doi: [10.1021/jp906296y](https://doi.org/10.1021/jp906296y)

40. Naseh MV, Khodadadi AA, Mortazavi Y, Pourfayaz F, Alizadeh O, Maghrebi M (2010) Fast and clean functionalization of carbon nanotubes by dielectric barrier discharge plasma in air compared to acid treatment. *Carbon* 48(5):1369–1379
41. Nativ-Roth E, Shvartzman-Cohen R, Bounioux C, Florent M, Zhang D, Szleifer I, Yerushalmi-Rosen R (2007) physical adsorption of block copolymers to SWNT and MWNT: a nonwrapping mechanism. *Macromolecules* 40(10):3676–3685. doi:[10.1021/ma0705366](https://doi.org/10.1021/ma0705366)
42. Hamley IW (2005) Block copolymers in solutions. Wiley, Chichester
43. Chu B, Zhou Z (1996) Physical chemistry of polyoxyalkylene block copolymer surfactants. In: Nace VM (ed) Nonionic surfactants: polyoxyalkylene block copolymers. Marcel Dekker, New York
44. Broersma S (1960) Rotational diffusion constant of a cylindrical particle. *J Chem Phys* 32(6): 1626–1631
45. Abraham TN, Debbatta R, Siengchin S, Karger-Kocsis J (2008) Rheological and thermal properties of poly(ethylene oxide)/multiwall carbon nanotube composites. *J Appl Polym Sci* 110(4):2094–2101
46. Chen H-W, Chang F-C (2001) The novel polymer electrolyte nanocomposite composed of poly(ethylene oxide), lithium triflate and mineral clay. *Polymer* 42(24):9763–9769
47. Valentini L, Biagiotti J, Kenny JM, Santucci S (2003) Morphological characterization of single-walled carbon nanotubes-PP composites. *Compos Sci Technol* 63(8):1149–1153
48. Assouline E, Lustiger A, Barber AH, Cooper CA, Klein E, Wachtel E, Wagner HD (2003) Nucleation ability of multiwall carbon nanotubes in polypropylene composites. *J Polym Sci Part B: Polym Phys* 41(5):520–527
49. Chatterjee T, Yurekli K, Hadjiev VG, Krishnamoorti R (2005) Single-walled carbon nanotube dispersions in poly(ethylene oxide). *Adv Funct Mater* 15(11):1832–1838